Article:

Choi, Jinho and Ko, Youngwook (2018) TCM for OFDM-IM. IEEE wireless communications letters. pp. 50-53. ISSN 2162-2337

https://doi.org/10.1109/LWC.2017.2752168

TCM for OFDM-IM

Jinho Choi and Youngwook Ko

***Abstract*—Orthogonal frequency division multiplexing (OFDM) with index modulation (IM) is a multicarrier transmission technique for frequency-selective fading channels. Although it is energy and spectral efficient, its performance may not be satisfactory as some active subcarriers can be suppressed by fading. In this letter, we consider trellis coded modulation (TCM) for OFDM-IM in order to improve the detection performance of active subcarriers by increasing the Hamming distance between index symbols. We devise mapping rules for TCM for two cases and it is shown that the diversity order can be improved, which results in a lower probability of index error.**

***Index Terms*—trellis coded modulation; index modulation; orthogonal frequency division multiplexing**

I. Introduction

In orthogonal frequency division multiplexing (OFDM), a subset of subcarriers can be active and their indices are used to convey additional information bits for index modulation (IM), which is called OFDM-IM [1] [2]. There have been various generalizations of OFDM-IM. For example, in [3], the number of active subcarriers is not fixed to increase the spectral efficiency. In [4], OFDM-IM is applied to multiple input multiple output (MIMO) systems. In [5], the optimal number of active subcarriers is studied to improve the spectral efficiency as well as energy efficiency. An overview of various IM techniques is presented in [6], [7] and a performance analysis is carried out when a maximum likelihood (ML) detector is employed in [8].

In general, OFDM-IM has a poor performance under fading. This is a weakness of OFDM-IM inherited from OFDM, which cannot exploit any diversity gain under a frequency-selective fading channel environment [9] [10]. In order to improve the performance of OFDM-IM, multiple antennas can be considered for OFDM-IM as in [4], [11]. It is also possible to consider a transmit diversity scheme without using multiple antennas as in [12], [13].

It is noteworthy that channel coding plays a crucial role in improving the performance of OFDM systems under a frequency-selective fading channel environment [14]. However, unlike coded OFDM, it is clearly shown in [12] that the direct application of channel coding to OFDM-IM cannot result in a good performance without a transmit diversity scheme. Thus, a transmit diversity scheme such as that in [12] or [15], which is a repetition diversity technique, is important for a reasonable performance of OFDM-IM.

Jinho Choi is with School of Electrical Engineering and Computer Science, Gwangju Institute of Science and Technology (GIST), Gwangju, 61005, Korea (Email: jchoi0114@gist.ac.kr). Youngwook Ko is with School of Electronics, Electrical Eng. and Computer Science, Queens University of Belfast, United Kingdom (Email: y.ko@qub.ac.uk). This work was supported by the "Climate Technology Development and Application" research project (K07732) through a grant provided by GIST in 2017.

In this letter, we study trellis coded modulation (TCM) [16] [17] for OFDM-IM. In particular, TCM is applied to IM so that the active subcarriers can be reliably detected. A pattern of active subcarriers in a cluster is seen as an index symbol. Unlike conventional TCM, the TCM symbol sequence is a sequence of the patterns of active subcarriers in the frequency domain and the length of sequence is the number of clusters. Mapping rules to decide a symbol from the output of a trellis code (i.e., convolutional code) are devised for two cases to maximize the Hamming distance as a performance criterion. Consequently, the increase of the distance between any pair of TCM symbol sequences results in a better detection performance of active subcarriers than that of uncoded cases. We can also show that the increase of the Hamming distance leads to the increase of diversity gain.

Notation: Matrices and vectors are denoted by upper- and lower-case boldface letters, respectively. The 2-norm of a vector $\mathbf{a}$ is denoted by $||\mathbf{a}||$. For a matrix $\mathbf{X}$ (a vector $\mathbf{a}$), $[\mathbf{X}]_n$ ($[\mathbf{a}]_n$) represents the nth column (element, resp.). If n is a set of indices, $[\mathbf{X}]_n$ is a submatrix of $\mathbf{X}$ obtained by taking the corresponding columns. $\mathcal{CN}(\mathbf{a}, \mathbf{R})$ ($\mathcal{N}(\mathbf{a}, \mathbf{R})$) represents the distribution of circularly symmetric complex Gaussian (CSCG) (resp., real-valued Gaussian) random vectors with mean vector $\mathbf{a}$ and covariance matrix $\mathbf{R}$.

II. System Model for TCM-OFDM-IM

A. System model

Suppose that there are $L = GN$ subcarriers, where G represents the number of cluster and N is the number of subcarriers per cluster. In each cluster, Q subcarriers are active, where $Q < N$, for OFDM-IM. Thus, the number of bits transmitted by index modulation per cluster becomes

$$B_{\rm C} = Q \log_2 M + B_{\rm I},$$

where $B_{\rm I} = \lfloor \log_2 \binom{N}{Q} \rfloor$ and M is the size of the signal constellation, denoted by $\mathcal{M}$, for the data symbols that are transmitted by active subcarriers. For convenience, the pattern of active subcarrier indices for each cluster is referred to as the cluster index (CI) symbol. For example, if $N = 5$ and $Q = 2$, there are $\binom{N}{Q} = \binom{5}{2} = 10$ CI symbols. Among those, we only use 8 symbols to represent 3 bits as $\lfloor \log_2 \binom{5}{2} \rfloor = 3$. In Table I, we show 8 CI symbols with $N = 5$ and $Q = 2$.

If some active subcarriers experience severe fading, the receiver may not be able to detect those active subcarriers and the performance becomes unsatisfactory in OFDM-IM. In order to overcome this problem, we can use channel coding. In particular, in this section, we consider TCM for OFDM-IM.

TCM is used to encode the bits delivered by IM. Let s_g denote the gth CI symbol in an OFDM-IM, $g = 0, \ldots, G-1$. As mentioned earlier, each CI symbol can deliver $B_{\rm I}$ bits. To

TABLE I
AN ILLUSTRATION OF 8 CI SYMBOLS FOR $N = 5$ AND $Q = 2$.

label (CI symbol)	pattern
1	[1 1 0 0 0]
2	[1 0 1 0 0]
3	[1 0 0 1 0]
4	[1 0 0 0 1]
5	[0 1 1 0 0]
6	[0 1 0 1 0]
7	[0 0 1 1 0]
8	[0 0 1 0 1]

TABLE II
THE SYMBOL MAPPING FOR THE TCM ENCODER IN FIG. 1.

c_0	c_1	c_2	CI symbol label
0	0	0	1
0	0	1	8
0	1	0	2
0	1	1	6
1	0	0	3
1	0	1	5
1	1	0	4
1	1	1	7

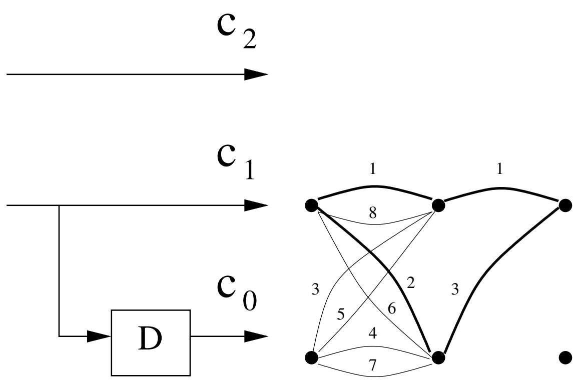

(a) (b)

Fig. 1. TCM scheme with a two-state trellis: (a) encoder ('D' in the box represents a delay unit); (b) trellis diagram (the pair of paths yielding the free distance is shown in bold)

apply TCM, we assume that B_I bits are decided by a TCM encoder. In this case, $\{s_g\}$ becomes an output sequence of a TCM encoder. For illustration purposes, we consider two design examples.

B. Design I

With $N = 5$ and $Q = 2$, consider a two-state TCM encoder that is shown in Fig. 1 (a) that has two bits for the input and three bits for the output. The corresponding trellis diagram is shown in Fig. 1 (b). Since c_2 is an uncoded bit, the trellis diagram has parallel transitions. The set of three bits, $\{c_0, c_1, c_2\}$, decides the CI symbol according to Table II. In this case, the number of bits (per cluster) delivered by IM becomes 2 bits, not $\lfloor \binom{5}{2} \rfloor = 3$ bits.

Let $d(n, m)$ denote the Hamming distance between CI symbols n and m. For example, according to Table I, $d(1, 2) = 2$, while $d(1, 8) = 4$. The free distance of TCM is the smallest distance between pairs of signals associated with parallel transitions or the smallest distance between pairs of paths diverging from a node and remerging after some instance. To see the free distance of TCM, we consider the CI symbols in Table I and a two-state TCM in Fig. 1. For a pair associated with parallel transitions (competing paths with length 1), we can have the Hamming distance as follows:

$$d(\{1, 8\}, \{1, 1\}) = d(1, 8) + d(1, 1) = 4 + 0 = 4.$$

On the other hand, for the case of competing paths with length > 1, we consider the path consisting of CI symbols 2 and 3 and the path of all CI symbol 1, which are shown in bold in Fig. 1. The Hamming distance of the two pairs is given by

$$d(\{1, 1\}, \{2, 3\}) = d(1, 2) + d(1, 3) = 2 + 2 = 4.$$

As a result, we can see that the two-state TCM in Fig. 1 has a free distance of 4.

Note that the free distance of uncoded cases (i.e., without TCM) is 2. For example, from Table I, if no TCM is used, we can see that the minimum Hamming distance between any pair of different CI symbols is 2. As in [15], a repetition diversity scheme can be considered. If the same CI symbol is used for two clusters, the minimum Hamming distance or free distance becomes 4. However, the spectral efficiency of IM[1] becomes halved (compared with uncoded systems), while the spectral efficiency of IM of the TCM scheme in Fig. 1 has decreased by a factor of $2/3$ with the same free distance, which is 4.

The transmitted signal vector of cluster g is given by

$$\mathbf{x}_g = \mathbf{a}(s_g, \mathbf{d}_g), \tag{1}$$

where $\mathbf{d}_g$ represents the vector of the data symbols that are transmitted by active subcarriers and $\mathbf{a}(s, \mathbf{d})$ represents the IM function with CI symbol s and data symbol vector $\mathbf{d}$. Clearly, the size of $\mathbf{d} = \mathbf{d}_g$ is $Q \times 1$ and each data symbol becomes a constellation point of $\mathcal{M}$. For example, suppose that $N = 5$ and $Q = 2$. According to Table I, if $s = 8$ and $\mathbf{d} = [d_1 \ d_2]^\mathrm{T}$, where $d_q \in \mathcal{M}$, we have $\mathbf{a}(s, \mathbf{d}) = [0 \ 0 \ d_1 \ 0 \ d_2]^\mathrm{T}$.

C. Design II

In order to increase the free distance, we can consider another design with $N = 4$ and $Q = 2$. Among $\binom{4}{2} = 6$ CI symbols, only the 4 CI symbols in Table III are chosen. With them, a TCM scheme can be considered with a rate-half convolutional encoder with generating polynomial $(5, 7)$ in octal. In this case, there are no parallel transitions and the four-state trellis diagram can be shown as in Fig. 2.

TABLE III
AN ILLUSTRATION OF THE 4 CI SYMBOLS FOR $N = 4$ AND $Q = 2$.

label (CI symbol)	pattern
1	[1 1 0 0]
2	[1 0 1 0]
3	[0 1 0 1]
4	[0 0 1 1]

[1]For this spectral efficiency, only IM bits are taken into account.

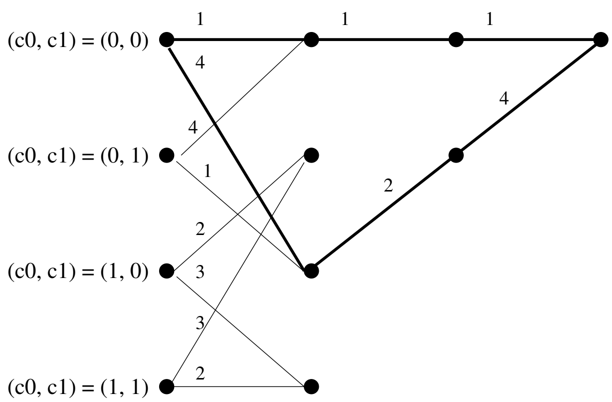

Fig. 2. A rate-$1/2$ 4-state TCM scheme for OFDM-IM (the pair of paths yielding the free distance is shown in bold).

According to Fig. 2, for the pair of the two paths, $\{1, 1, 1\}$ and $\{4, 2, 4\}$, we can see that the Hamming distance becomes $d(\{1, 1, 1\}, \{4, 2, 4\}) = 2d(1, 4) + d(1, 2) = 8 + 2 = 10$. This TCM has a rate of $1/2$ as a single bit becomes two coded bits that decide the pattern of active subcarriers in a cluster. Clearly, we can have a larger Hamming distance at the cost of the spectral efficiency.

As in [15], it is possible to use repetition diversity for reliable transmissions of IM bits. For example, the same set of active subcarriers can be used for two clusters, which results in a diversity order of 4 or a free distance of 4 at the cost of the spectral efficiency. Compared to the above rate-half TCM, the gain of repetition diversity (in terms of the free distance) is small.

III. ML Decoding for TCM-OFDM-IM

In this section, we study the ML decoding for TCM-OFDM-IM. Let $\mathbf{H}_g$ represent the (frequency-domain) diagonal channel matrix for cluster g in OFDM-IM. The received signal vector at the gth cluster is given by

$$\mathbf{r}_g = \mathbf{H}_g \mathbf{x}_g + \mathbf{n}_g = \mathbf{H}_g \mathbf{a}(s_g, \mathbf{d}_g) + \mathbf{n}_g, \tag{2}$$

where $\mathbf{x}_g$ and $\mathbf{n}_g \sim \mathcal{CN}(\mathbf{0}, N_0 \mathbf{I})$ represent the transmitted signal vector and the background noise at the gth cluster, respectively. Then, the ML detection is to find $\{s_g, \mathbf{d}_g\}$ that maximizes the following likelihood function:

$$f(\{\mathbf{r}_g\}|\{s_g, \mathbf{d}_g\}) = \prod_{g=0}^{G-1} \exp\left(-\frac{||\mathbf{r}_g - \mathbf{H}_g \mathbf{a}(s_g, \mathbf{d}_g)||^2}{N_0}\right).$$

The log-likelihood function of $\{s_g, \mathbf{d}_g\}$ is given by

$$C(s_0, \ldots, s_{G-1};, \mathbf{d}_0, \ldots, \mathbf{d}_{G-1}) = \sum_{g=0}^{G-1} C_g(s_g; \mathbf{d}_g), \tag{3}$$

where $C_g(s; \mathbf{d}) = ||\mathbf{r}_g - \mathbf{H}_g \mathbf{a}(s, \mathbf{d})||^2$. Since the data symbol vectors, $\mathbf{d}_g$, are independent of TCM, the cost function for TCM decoding using the Viterbi algorithm[2] [18] can be given by

$$C(s_0, \ldots, s_{G-1}) = \sum_{g=0}^{G-1} C_g(s_g), \tag{4}$$

where

$$C_g(s) = \min_{\mathbf{d} \in \mathcal{M}^Q} ||\mathbf{r}_g - \mathbf{H}_g \mathbf{a}(s, \mathbf{d})||^2. \tag{5}$$

In (5), it is implied that the data symbols are detected for given CI symbol (or given set of active subcarriers) in each cluster.

On the other hand, if $\mathbf{d}_g$ is known or fixed, we have

$$C_g(s) = ||\mathbf{r}_g - \mathbf{H}_g \mathbf{a}(s, \mathbf{d}_g)||^2. \tag{6}$$

In this case, the probability of index error or CI symbol error is decided by the free distance. Particularly, we can consider the average pairwise error probability (PEP) for CI symbol detection for a given cluster (for convenience, we omit the cluster index g) when s is the correct CI symbol:

$$P(s \to s') = \Pr\left(||\mathbf{r} - \mathbf{H}\mathbf{a}(s, \mathbf{d})||^2 > ||\mathbf{r} - \mathbf{H}\mathbf{a}(s', \mathbf{d})||^2\right), \tag{7}$$

where $s' \neq s$. If the diagonal elements of $\mathbf{H}$ are independent CSCG with zero-mean and unit variance, from [19] [18], we have

$$P(s \to s') \leq \left(\frac{1}{1 + \frac{E_{\mathrm{s}}}{N_0}}\right)^{d_{\mathrm{H}}(s, s')}, \tag{8}$$

where $d_{\mathrm{H}}(s, s')$ denotes the Hamming distance between CI symbols s and s' and E_{s} is the symbol energy of active subcarrier. The average PEP in (8) clearly shows that TCM can improve the performance of OFDM-IM in terms of the index detection of active subcarriers and the design criterion has to be the Hamming distance between CI symbols.

IV. Simulation Results

In this section, we present simulation results when the frequency-domain channel coefficients are CSCG random variables as $h_{n,g} \sim \mathcal{CN}(0, 1)$, where $h_{n,g}$ denotes the channel coefficient corresponding to nth subcarrier of cluster g, i.e., $[\mathbf{H}_g]_{n,n} = h_{n,g}$. The signal-to-noise ratio (SNR) is defined by $\frac{E_{\mathrm{b}}}{N_0}$, where E_{b} represents the bit energy. In particular, the bit energy in this section is only for IM bits, which is given by $E_{\mathrm{b}} = \frac{QE_{\mathrm{s}}}{B_{\mathrm{I}} r_{\mathrm{tcm}}}$, where E_{s} is the symbol energy of active subcarrier and r_{tcm} is the rate of the TCM encoder. We consider the two TCM-OFDM-IM schemes. The first scheme is based on the rate-$2/3$ TCM with two-state that is illustrated in Fig. 1 with $(N, Q) = (5, 2)$. The second scheme is based on the rate-$1/2$ TCM with four-state that is illustrated in Fig. 2 with $(N, Q) = (4, 2)$.

Fig. 3 shows the bit error rates (BERs) of uncoded OFDM-IM and the two TCM-OFDM-IM schemes when $\mathbf{d}_g$ is fixed (i.e., the elements of $\mathbf{d}_g$ are assumed to be 1). For ML decoding, in this case, the cost of each cluster g is (6). It can be shown that the diversity order of uncoded OFDM-IM is 2 and that of the rate-$2/3$ TCM scheme is 4 as expected. In other words, the diversity order is identical to the free distance. The rate-$1/2$ TCM scheme outperforms the others as its free distance is larger than those of the others, which is 10.

[2] Its complexity is proportional to the product of the length of coded sequence, G, and $|\mathcal{M}|^Q$.

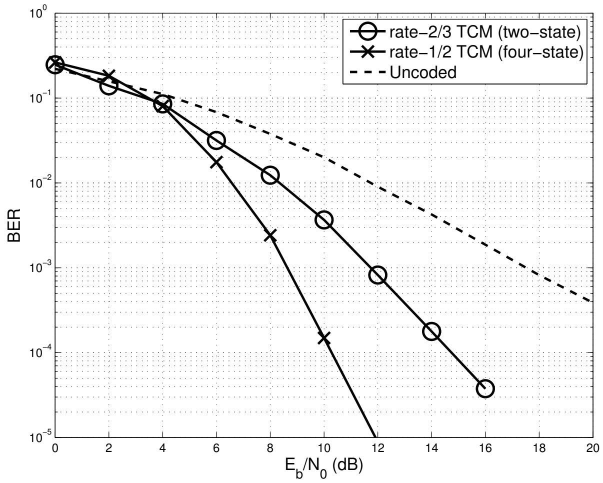

Fig. 3. BER versus E_{b}/N_0 of uncoded OFDM-IM and TCM-OFDM-IM systems (rate-2/3 TCM with 2-state and $(N, Q) = (5, 2)$ and rate-$1/2$ TCM with 4-state and $(N, Q) = (4, 2)$) when the data symbols are fixed and known at the receiver (i.e., $\mathbf{d}_g = \mathbf{1}$).

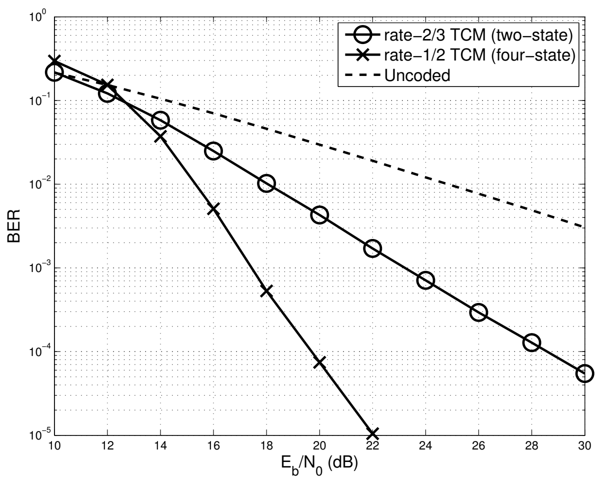

Fig. 4. BER versus E_{b}/N_0 of uncoded OFDM-IM and TCM-OFDM-IM systems (rate-2/3 TCM with 2-state and $(N, Q) = (5, 2)$ and rate-$1/2$ TCM with 4-state and $(N, Q) = (4, 2)$) when QAM is used for $\mathbf{d}_g \in \mathcal{M}^Q$, where $\mathcal{M} = \{(\pm 1 \pm j)/\sqrt{2}$.

We now consider the case that the data symbols are not fixed. For ML decoding, the cost of each cluster g is (5). Compared with the results in Fig. 3, we can see that the BERs in Fig. 4 are high due to the detection errors of data symbols. More importantly, we can observe that the diversity order has decreased. For example, from the BER result in Fig. 4, we can see that the diversity order of the rate-$2/3$ TCM scheme is about 2 (as the SNR at a BER of 10^{-2} is 18 dB, while that at a BER of 10^{-3} is about 23 dB). On the other hand, its free distance is 4 and the diversity order in Fig. 3 is also shown to be 4. To see the performance (with data symbol detection) clearly, we need a further study in the future.

V. Conclusions

TCM has been applied to CI symbols in OFDM-IM in order to increase the Hamming distance between CI sequences, which results in a better detection performance over frequency-selective fading channels. We devised two designs for TCM-OFDM-IM and showed the increase of the free distance. It was also shown that the maximization of Hamming distance results in the decrease of the probability of index error as the diversity gain increases. Simulations have been carried out to see the performances of the two designed mapping rules for TCM-OFDM-IM.

As further research topics, we consider a generalized design rule for TCM-OFDM-IM and a complete performance analysis with data symbol detection, which can allow us to see the relationship between the diversity gain and the free distance of TCM clearly.

References

[1] R. Abu-alhiga and H. Haas, "Subcarrier-index modulation OFDM," in *Personal, Indoor and Mobile Radio Communications, 2009 IEEE 20th International Symposium on*, pp. 177–181, Sept 2009.

[2] E. Basar, U. Aygolu, E. Panayirci, and H. Poor, "Orthogonal frequency division multiplexing with index modulation," *IEEE Trans. Signal Processing*, vol. 61, pp. 5536–5549, Nov 2013.

[3] R. Fan, Y. J. Yu, and Y. L. Guan, "Generalization of orthogonal frequency division multiplexing with index modulation," *IEEE Trans. Wireless Communications*, vol. 14, pp. 5350–5359, Oct 2015.

[4] E. Basar, "Multiple-input multiple-output OFDM with index modulation," *IEEE Signal Processing Letters*, vol. 22, pp. 2259–2263, Dec 2015.

[5] W. Li, H. Zhao, C. Zhang, L. Zhao, and R. Wang, "Generalized selecting sub-carrier modulation scheme in OFDM system," in *2014 IEEE International Conference on Communications Workshops (ICC)*, pp. 907–911, June 2014.

[6] E. Basar, "Index modulation techniques for 5G wireless networks," *IEEE Communications Magazine*, vol. 54, pp. 168–175, July 2016.

[7] N. Ishikawa, S. Sugiura, and L. Hanzo, "Subcarrier-index modulation aided OFDM - will it work?," *IEEE Access*, vol. 4, pp. 2580–2593, 2016.

[8] Y. Ko, "A tight upper bound on bit error rate of joint OFDM and multi-carrier index keying," *IEEE Communications Letters*, vol. 18, pp. 1763–1766, Oct 2014.

[9] Y. S. Cho, J. Kim, W. Y. Yang, and C. G. Kang, *MIMO-OFDM Wireless Communications with MATLAB*. Wiley-IEEE Press, 2010.

[10] J. Choi, *Adaptive and Iterative Signal Processing in Communications*. Cambridge University Press, 2006.

[11] J. Crawford, E. Chatziantoniou, and Y. Ko, "On the sep analysis of ofdm index modulation with hybrid low complexity greedy detection and diversity reception," *IEEE Trans. Veh. Technol.*, vol. PP, April 2017.

[12] E. Basar, "OFDM with index modulation using coordinate interleaving," *IEEE Wireless Communications Letters*, vol. 4, pp. 381–384, Aug 2015.

[13] T. V. Luong and Y. Ko, "A closed-form symbol error probability for MCIK-OFDM with frequency diversity," in *Proc. IEEE SPAWC*, pp. 1–5, Jul 2017.

[14] H. Sari, G. Karam, and I. Jeanclaude, "Transmission techniques for digital terrestrial TV broadcasting," *IEEE Communications Magazine*, vol. 33, pp. 100–109, Feb 1995.

[15] J. Choi, "Coded OFDM-IM with transmit diversity," *IEEE Trans. Communications*, vol. 65, pp. 3164–3171, July 2017.

[16] G. Ungerboeck, "Channel coding with multilevel/phase signals," *IEEE Trans. Information Theory*, vol. 28, pp. 55–67, Jan 1982.

[17] G. Ungerboeck, "Trellis-coded modulation with redundant signal sets part I: Introduction," *IEEE Communications Magazine*, vol. 25, pp. 5–11, February 1987.

[18] E. Biglieri, *Coding for Wireless Channels*. New York: Springer, 2005.

[19] S. H. Jamali and T. Le-Ngoc, *Coded Modulation Techniques for Fading Channels*. Kluwer Academic Publishers, 1994.